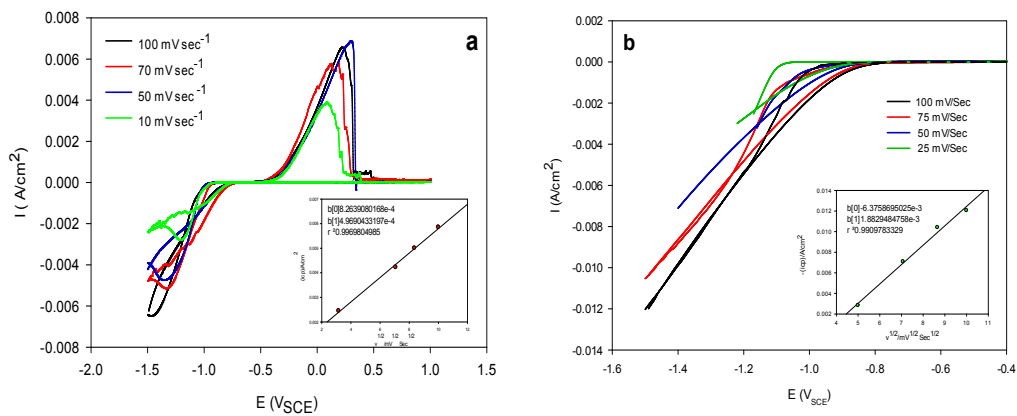
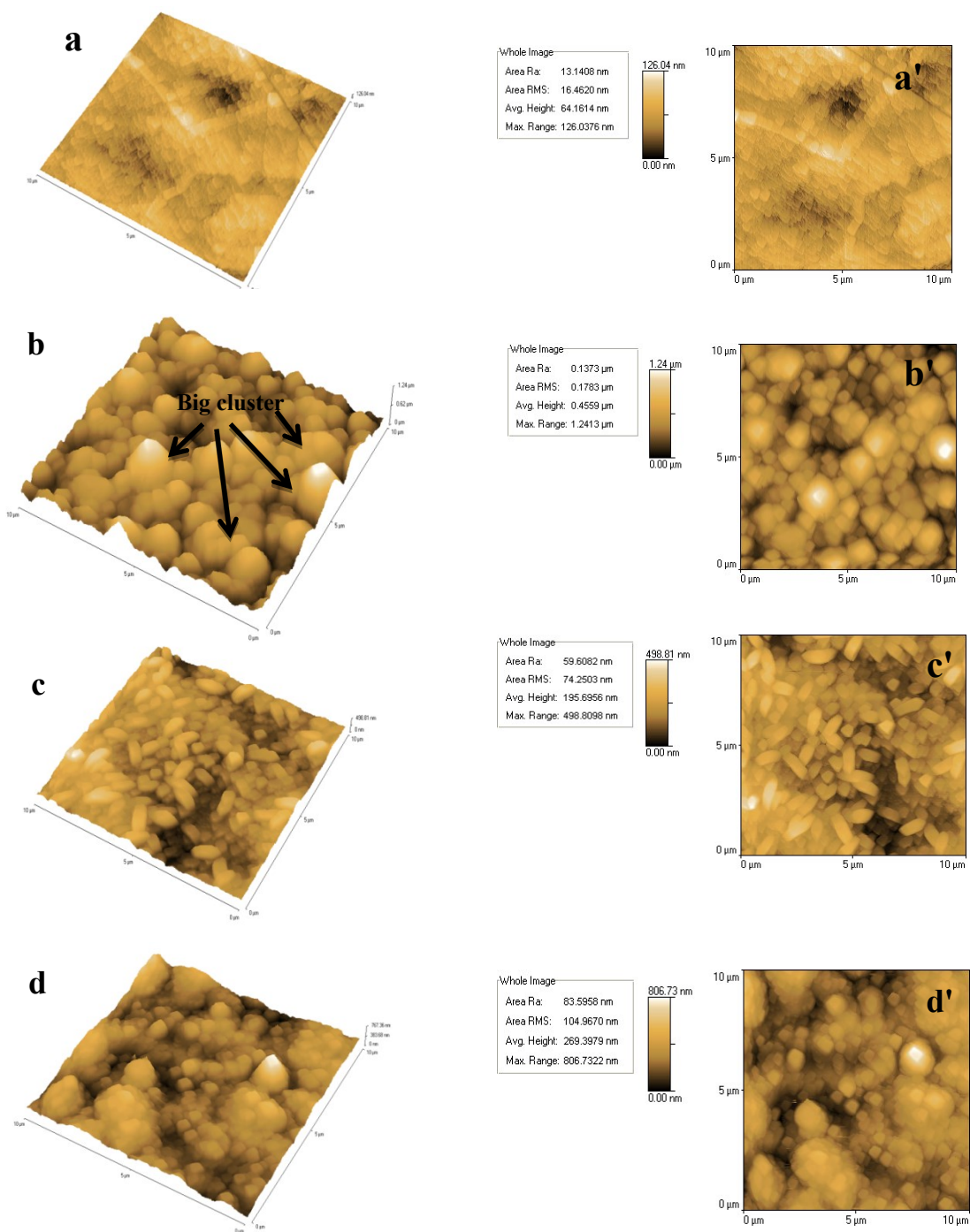


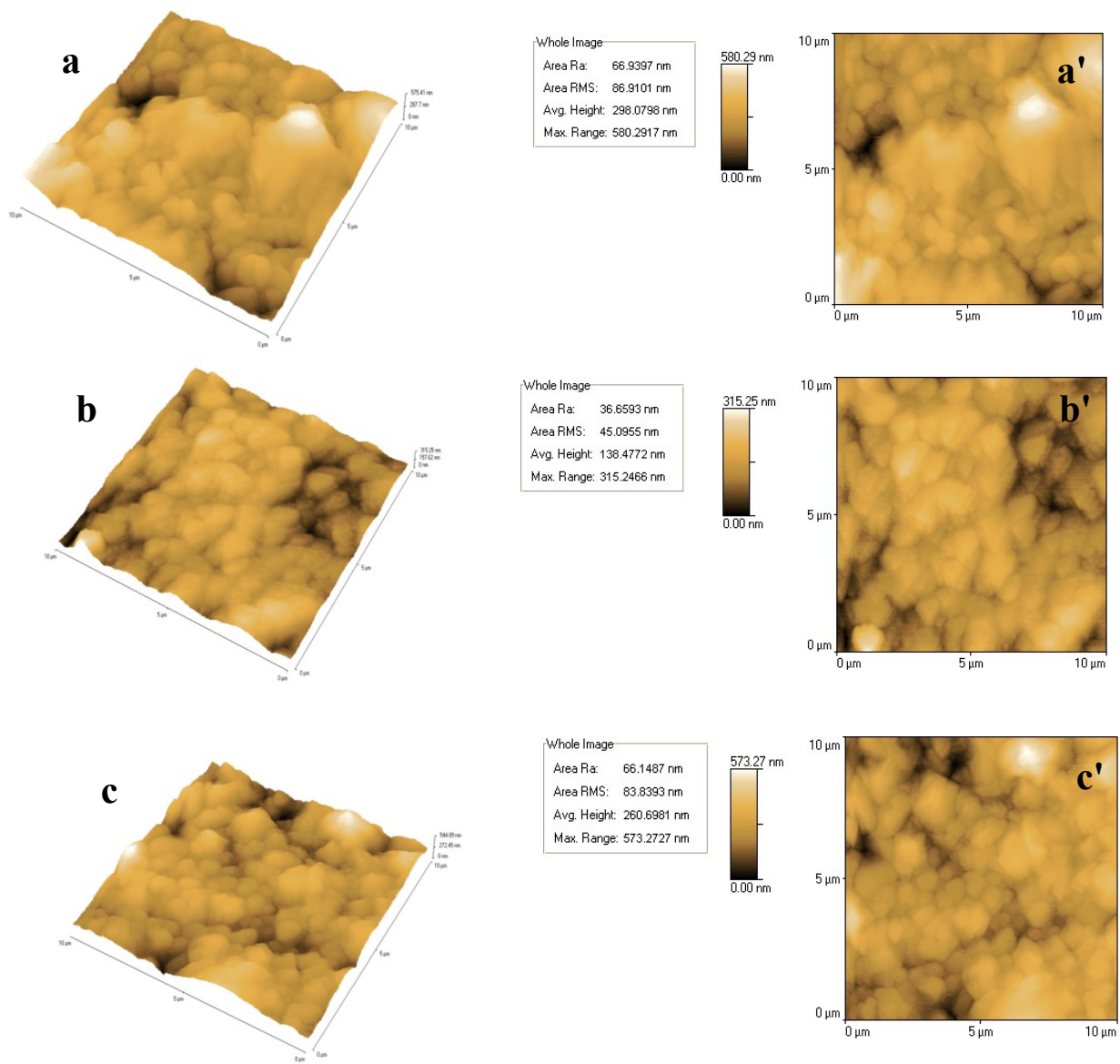
**S1.** Plot of  $\theta/(1-\theta)$  vs concentration of Im-IL: (a) Co (b) Ni electrodeposition.



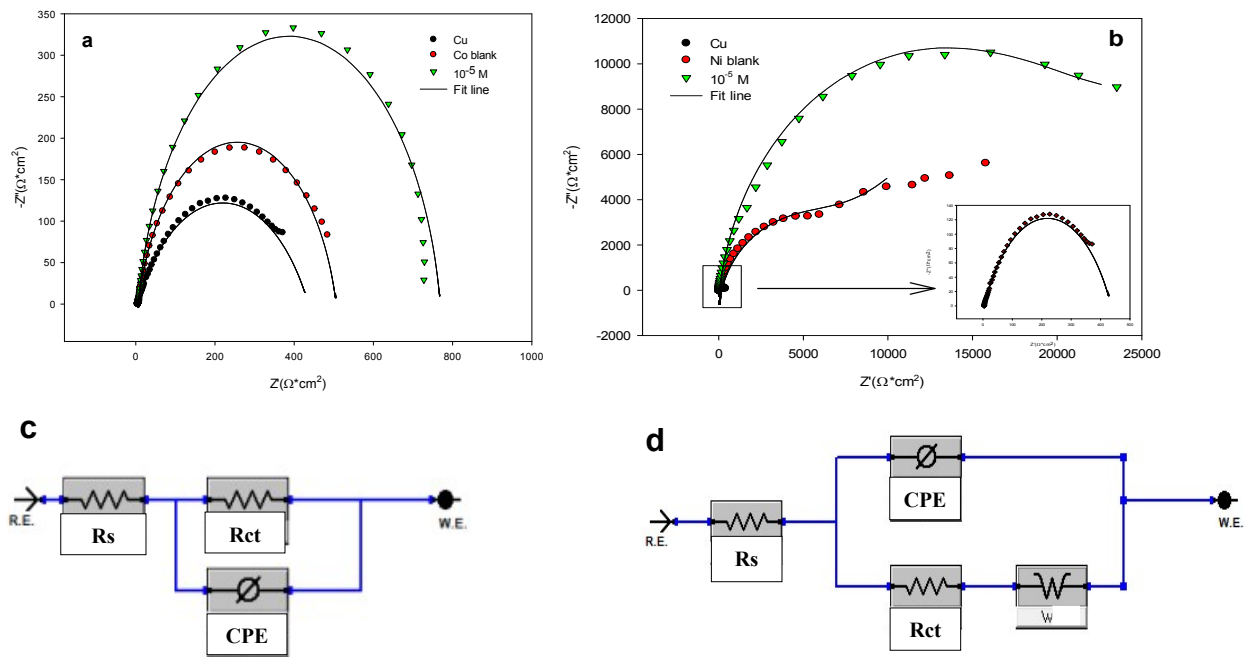
**S2.** CVs for (a) Co and (b) Ni electrodeposition at  $1 \times 10^{-5}$  M Im-IL recorded at GCE with different scan rates. Insert linear relation between cathodic peak current density ( $i_{cp}$ ) as a function of the scan potential rate  $v^{1/2}$ .



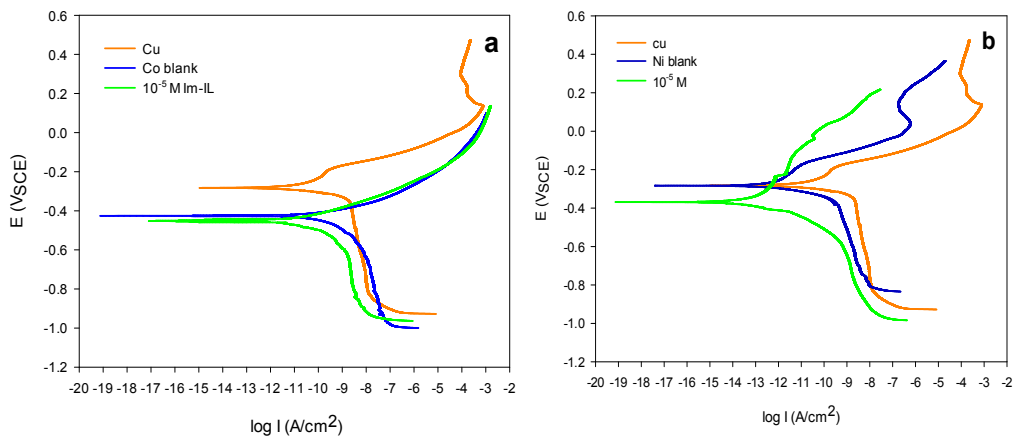
**S3.** AFM 3D, 2D images, of (a, a') pure copper (substrate), Co deposited from bath (b, b') free-Im-IL, (c, c')  $1 \times 10^{-5}$  M Im-IL, (d, d')  $1 \times 10^{-3}$  M Im-IL.



**S4.** AFM 3D, 2D images, of Ni deposited from bath (a, a') free-Im-IL, (b, b')  $1 \times 10^{-4}$  M Im-IL ,(c, c')  $5 \times 10^{-6}$  M Im-IL.



**S5.** Nyquist plots for Cu substrate (a) Co and (b) Ni deposits in 3.5% NaCl in the absence and presence of  $1 \times 10^{-5}$  M Im-IL. Equivalent circuit compatible with the experimental impedance data (c) Co, (d) Ni deposits.



**S6.** Potentiodynamic polarization curves for Co and Ni deposits in the absence and presence of  $1 \times 10^{-5}$  M Im-IL in 3.5% NaCl.

**T1** CPP of Co and Ni electrodeposition at  $2.0 \times 10^{-3}$  mA.cm<sup>-2</sup> in the absence and presence of different concentrations of Im-IL and  $\theta$  by Im-IL at different concentrations.

[Im-IL] (M)	(CPP) Co $V_{SCE}$	$\theta$ (Co)	(CPP) Ni $V_{SCE}$	$\theta$ (Ni)
0.0	-0.82	-	-0.97	-
$1.0 \times 10^{-6}$	-0.84	0.0481	-1.00	0.396
$1.0 \times 10^{-5}$	-0.85	0.0531	-1.01	0.423
$5.0 \times 10^{-5}$	-	-	-1.04	0.520
$1.0 \times 10^{-4}$	-0.88	0.0714	-1.24	0.724
$5.0 \times 10^{-4}$	-	-	-1.45	0.866
$1.0 \times 10^{-3}$	-0.92	0.219	-	-

**T2** NOP and the height of anodic current ( $i_a$ ) peaks of ALSVs for Co and Ni electrodeposition in the absence and presence of different concentrations of Im-IL.

[Im-IL]/ M	NOP / mV (Co)	Height of $i_a$ peak (Acm <sup>-2</sup> )	NOP / mV (Ni)	Height of $i_a$ peak (Acm <sup>-2</sup> )
0	0.29	$4.57 \times 10^{-2}$	0.52	$4.17 \times 10^{-4}$
$1 \times 10^{-6}$	0.32	$3.84 \times 10^{-2}$	0.59	$4.06 \times 10^{-4}$
$1 \times 10^{-5}$	0.39	$2.58 \times 10^{-2}$	0.62	$3.40 \times 10^{-4}$
$5 \times 10^{-5}$	-	-	0.66	$1.66 \times 10^{-4}$
$1 \times 10^{-4}$	0.4	$1.08 \times 10^{-2}$	0.60	$9.65 \times 10^{-5}$
$5 \times 10^{-4}$	0.5	-	0.70	$2.52 \times 10^{-6}$
$1 \times 10^{-3}$	0.6	$5.34 \times 10^{-2}$	-	-



**T3** CCE%, Co and Ni deposits appearance under optimal bath conditions in absence and presence of different concentrations of Im-IL.

[Im-IL] (M)	CCE%		Deposition Appearance	
	(Co)	(Ni)	(Co)	(Ni)
0	99	99	Pale, hollow gray	Bright silver
$5 \times 10^{-7}$	98	97	Pale gray	Bright silver with little tiny pits
$1 \times 10^{-6}$	99	97	Pale gray	Bright silver with little tiny pits
$5 \times 10^{-6}$	-	98	Pale gray	Bright silver with many small pits
$1 \times 10^{-5}$	99.8	99	Bright gray	Bright silver with many small pits
$5 \times 10^{-5}$	-	99.6	-	Very bright silver with very small pits
$1 \times 10^{-4}$	99.5	99.8	Bright gray with little crack	Very bright silver with no pits
$5 \times 10^{-4}$	-	103	-	Very bright silver with no pits
$1 \times 10^{-3}$	104	-	Bright gray with more crack	-

**T4** The results from impedance and polarization measurements in 3.5% NaCl and average microhardness for the both Co and Ni deposits with and without Im-IL at 25°C.

	$R_{ct}$ ( $k\Omega \cdot cm^2$ )	CPE ( $k\Omega^{-1} S^n cm^{-2}$ )	IE%	W ( $k\Omega^{-1} S^{0.5} cm^{-2}$ )	$i_{corr}$ ( $\mu A cm^{-2}$ )	$-E_{corr}$ ( $mV_{SCE}$ ) $\times 10^{-1}$	Average Hardness ( $H_{V100}$ )
Cu	432.4	$553.7 \times 10^{-6}$	-	-	$2.84 \times 10^{-5}$	2.80	-
Co blank	500.1	$318.4 \times 10^{-6}$	-	-	$5.51 \times 10^{-6}$	4.26	342.5
$1 \times 10^{-5}$ (M)	2184	$1.109 \times 10^{-4}$	77.1	-	$9.71 \times 10^{-7}$	4.52	368.5
Ni blank	$7.26 \times 10^3$	$181.9 \times 10^{-6}$	-	$627 \times 10^{-6}$	$6.36 \times 10^{-6}$	2.83	211.25
$1 \times 10^{-5}$ (M)	$22.3 \times 10^3$	$122.8 \times 10^{-6}$	67.5	$528 \times 10^{-6}$	$3.21 \times 10^{-6}$	3.69	270